Zinc oxide and expandable graphite-based flame retardant coatings of unsaturated polyester resin for composite applications

Csvila P., Kovács Zs., Toldy A., Czigány T.

Accepted for publication in Journal of Vinyl & Additive Technology
Published in 2025
DOI: https://doi.org/10.1002/vnl.70055

Zinc Oxide and Expandable Graphite–Based Flame Retardant Coatings of Unsaturated Polyester Resin for Composite Applications

Csvila P.[1], *Kovács Zs*[1,2]., *Toldy A.*[1,2], *Czigany T.*[1,3*]

[1]*Budapest University of Technology and Economics, Faculty of Mechanical Engineering, Department of Polymer Engineering, Műegyetem rkp. 3., H-1111 Budapest, Hungary*

[2]*MTA-BME Lendület Sustainable Polymers Research Group, H-1111, Budapest, Műegyetem rkp. 3, Hungary*

[3]*HUN-REN-BME Research Group for Composite Science and Technology, Budapest University of Technology and Economics, Műegyetem rkp. 3., H-1111 Budapest, Hungary*

**corresponding author: czigany@eik.bme.hu*

Abstract

Halogen-free multifunctional composite coatings modified with zinc oxide (ZnO) and expandable graphite (EG) on glass fibre–reinforced unsaturated polyester (UPR) composites, developed for applications in electronics and other areas where local heat loads and mechanical stress can affect the composite surface, were investigated. The primary objective of the coatings was to provide mechanical protection and enhanced flame retardancy without the use of halogen-based flame retardants. The combined use of ZnO and EG reduced the maximum average rate of heat emission by 64% compared to the reference (465 kW/m^2). Furthermore, the effective heat of combustion was reduced from 3156 MJ/kg to 41 MJ/kg with the combined use of the flame retardands. In glow wire flammability index tests, the ignition temperature increased by 310 °C compared to the uncoated composite. When ZnO and EG were used together, a stable, intumescent char layer formed that effectively protected the substrate under local heat stress. The additives did not influence the adhesion of the coatings, while the combined ZnO–EG system demonstrated higher toughness and better crack dispersion under bending loads, maintaining coating integrity even after local deformation. These results indicate that halogen-free ZnO–EG coatings can provide both flame retardancy and mechanical robustness, making them promising for structural and electrical composite components exposed to heat and mechanical stress.

Highlights

- ZnO and EG form a stable heat barrier as fire-retardant coating
- The combined use of ZnO and EG reduced the total smoke production by 71%
- During burning, ZnO forms a stable ZnO-rich char layer on the surface
- ZnO and EG together give the coating higher stress resistance than alone
- The combined use of ZnO and EG reduced the peak heat release rate by 61%

Keywords

coating, flame retardant system, unsaturated polyester resin, glass fiber

1. Introduction

Polymer composites are widely used for their excellent strength-to-weight ratio, corrosion resistance, and processability in fields such as construction, automotive, marine, and electronics. However, their performance often depends on surface properties, which are commonly enhanced by coatings. Coatings improve appearance, hardness, wear and environmental resistance, and can add functionalities such as flame retardancy[1] [2] [3].

Reducing flammability is a critical issue for polymer matrix composites, as their material properties make them highly susceptible to rapid flame spread, intense smoke generation, and toxic gas emissions. One of the most commonly used polymer matrices is unsaturated polyester resin (UPR), which is widely used in the composite industry due to its low cost, good processability and chemical resistance, and excellent adhesion [4]. However, UPR is flammable, its thermal decomposition starts at about 280 °C, with the main degradation occurring between 400–430 °C, and its combustion is characterized by significant smoke release during cone calorimetry measurements, which is harmful to health and the environment [5]. Pure UPR-based composites often do not comply with the fire safety regulations required for industrial applications, therefore the use of flame retardants is necessary for their safe application [6].

Traditionally, in the electronics industry, halogen-containing flame retardants have been widely used in UPRs due to their effectiveness because they produce active free radicals during combustion, which are capable of deteriorating the combustion characteristics of the polymer matrix. However, despite their effectiveness, their use has now been restricted because they release toxic gases [7]. In the European Union, regulatory measures have increasingly limited the use of halogen-based flame retardants. The European Chemicals Agency (ECHA) has proposed, in its 2023 strategy, broad restrictions on halogenated compounds, particularly aromatic brominated species, due to their persistence, bioaccumulation, and toxicity, thereby promoting the transition towards halogen-free alternatives [8]. As a result, halogen-free flame retardants are now the main focus of research. One possible option is to use inorganic fillers, like aluminum hydroxide, magnesium hydroxide, or zinc oxide. The use of these fillers is not harmful to health, but they can only be used effectively for flame retardancy in large quantities, which has a negative impact on the mechanical properties and processability of the polymer [9]. For example, Jiao et al. [10] reported in their study that the addition of 50 m/m% magnesium hydroxide to ethylene-vinyl acetate (EVA) increased the limiting oxygen index (LOI) by 54%, reduced the peak heat release rate by 31%, and extended the time to ignition by 66%. However, it also decreased the tensile strength by 41% and, quite substantially, the elongation at break by 71%. Another solution for halogen-free flame retardants is intumescent flame retardants, which create an insulating char layer on the surface of the polymer under the effect of heat, protecting the polymer from further damage and thus improving its fire safety [11].

In crosslinked UPRs, conventional intumescent flame retardants are often ineffective, as the low char yield, high volatile release, and lack of polymer softening hinder the formation of a stable protective char layer. Expandable graphite (EG) offers a solution to this problem, as it can form an effective foam layer even in crosslinked materials. Mazela et al. [12] proved that since EG can expand up to 100 times its original size, it can form a much larger and more effective protective layer on the surface of the polymers than most intumescent flame retardants, when used in crosslinked polymers. Furthermore, EG is the only foamed char former that can expand with sufficient force to be an effective intumescent flame retardant in rigid, crosslinked systems such as phenolic resins. EG consists of graphite flakes intercalated with an acid (typically sulfuric acid), which undergo rapid exfoliation at high temperatures (approximately 200–300 °C), expanding to many times larger than its original volume, forming a thick, multi-cellular carbon foam. The carbon foam prevents oxygen from reaching the polymer and reduces the rate of further heat transfer, thereby slowing down or preventing the polymer product from burning and reducing smoke generation during combustion [13] [14].

However, EG alone creates a less stable combustion residue structure, which can easily disintegrate even under minor external forces, so it is advisable to combine it with other materials capable of forming a more stable carbon layer. One solution is to use various metal oxides, such as zinc oxide (ZnO). Deng et al. [15] investigated the effect of ZnO when used in combination with intumescent flame retardants. They demonstrated that ZnO reduced heat release, slowed down and controlled the combustion process, and resulted in a far stronger and more durable char residue. They explained this by saying that ZnO acts as a catalytic synergist during combustion, which promotes interactions between the intumescent flame retardant components and strengthens the resulting char, forming a more stable and cohesive protective layer [16] [17].

In the case of composite structures, fire retardancy—especially the use of intumescent fire retardants—poses significant challenges, as the expansion of intumescent fire retardants due to heat causes the layers of the composite structure to disintegrate, compromising the structural integrity of the composite in the event of a fire. This delamination reduces the mechanical properties and effectiveness of fire protection, as charring occurs in an uncontrolled manner inside the composite. Another problem is the so-called "filter effect", in which the flame retardant particles are often filtered out of the matrix by the reinforcing material, causing unequal distribution. To effectively solve these problems, the composite industry often uses a surface-applied, independent fire-retardant coating, which allows the intumescent system to act externally on the surface of the composite without significantly damaging the internal structure [18,19]. Multifunctional coatings are mainly used to improve the aesthetic appearance and provide mechanical protection for the polymer composites. However, without adequate adhesion, the coating may peel off, exposing the composite to mechanical and thermal loads [1].

Although several studies have reported the use of expandable graphite (EG) as a flame retardant in unsaturated polyester resin (UPR) [20], sometimes in combination with other types of flame retardant additives[21, 22], the flame-retardant and char-forming effects of ZnO are also well known [23]. However, the combined application of these two flame retardants and their mutual interactions have not yet been investigated.In this article, we investigated the effect of halogen-free ZnO and EG on the thermal and flammability properties, as well as the hardness and porosity of UPR. We also produced glass fiber–reinforced UPR composites with a UPR-based flame retardant coating on their surface. We analyzed the flammability of the coated composites using cone calorimetry and a glow wire flammability index test, and determined the adhesion between the coating and the composite surface. Finally, we examined the mechanical properties of the coated composites using a three-point bending test.

The motivation for developing such multifunctional coatings lies in their potential application in composite structures where both flame retardancy and mechanical integrity are required. Typical examples include electrical panels and housings, vehicle and aircraft components, and building facade or interior panels. In these areas, surface coatings that can simultaneously resist ignition, reduce heat release, and maintain structural integrity under thermal and mechanical stress are highly desirable. Therefore, the results of this study may contribute to the design of halogen-free, environmentally friendly protective coatings for composites operating under demanding thermal and mechanical conditions.

2. Materials and methods

2.1. Materials

During the tests, we used unsaturated polyester resin as matrix material in both the composite and the coating, which was prepared from Distitron 5119 ESX20ZQ unsaturated polyester resin (UPR, Polynt Composites Poland Sp. z o.o., Niepołomice, Poland) and a methyl ethyl ketone peroxide–based Peroxan ME 50 LX (PERGAN GmbH, Bocholt, Germany) polyester catalyst in a ratio of 100:1. After mixing, they were crosslinked at room temperature for 24 hours, then post-cured in two stages, first for 2 hours at 100 °C, then for 1 hour at 100 °C.

The reinforcing material used in the composites was glass fabric with a specific weight of 220 g/m^2 (GF, UNIQUE Textiles, s.r.o., Fryšták, Czech Republic). No further treatment was applied to the glass fabric during lamination.

In the flame-retardant coating, we used zinc oxide with a minimum purity of 99% (ZnO, Molar Chemicals Kft., Halásztelek, Hungary) with a median particle size of 0.795 µm and 90% of the particles below 2.88 µm and expandable graphite (Graphit Kropfmühl, Hauzenberg, Germany), 75% of which had a particle size of less than 150 µm, an expansion rate of 100 cm^3/g and the carbon content minimum 92%.

2.2. Methods of preparation

For a more accurate examination of the coated composites (Figure 1b), we also examined the coatings of the UPR matrix on their own (Figure 1a).

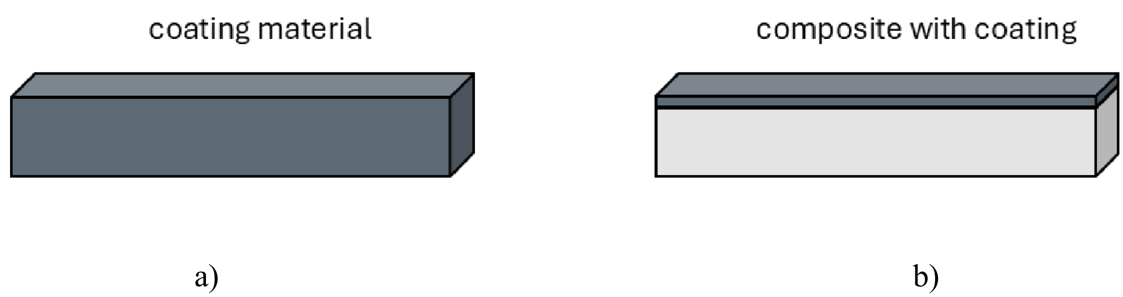

Figure 1: The samples examined were a) test specimens made from the coating material only, b) test specimens made from the coated composite material.

Table 1 summarizes the names of the test specimens produced from the coating materials and the quantities of particles used in them.

Table 1: Description of samples prepared from coatings, additive content and type

Sample name	ZnO content (m/m%)	EG content (m/m%)
UPR	0	0
UPR/ZnO	30	0
UPR/EG	0	5
UPR/ZnO/EG	30	5

Table 2 shows the names of the coated composite test specimens and the quantities of particles used in their coatings.

Table 2: Names of coated composite samples, additive content and type of coatings.

Sample name	ZnO content in the coating (m/m%)	EG content in the coating (m/m%)
UPR/GF	-	-
UPR/GF+UPR_ctg	0	0
UPR/GF+ZnO_ctg	30	0
UPR/GF+EG_ctg	0	5
UPR/GF+EG/ZnO_ctg	30	5

During the preparation of the coatings (Figure 2), ZnO and EG particles were mixed into the UPR matrix monomer, which was first dispersed by mechanical mixing for 5 minutes, followed by ultrasonic mixing at 20 kHz and 100 W for 3 minutes to improve the uniform distribution of the particles. During ultrasonic homogenization, the temperature of the suspension was kept below 60°C with a cooling bath. A Bandelin Sonopuls 4200 HD UH homogenizer (BANDELIN Electronic GmbH & Co. KG, Berlin, Germany) was used for ultrasonic mixing.

To examine the coatings described in Table 1, we produced coating specimens by casting in a silicone mold. The test specimens had dimensions of 120 mm x 10 mm x 4 mm for the UL 94 test and 100 mm x 100 mm x 4 mm for the cone calorimetry test. To produce the flame-retardant coated composites shown in Table 2, we first produced a 3 mm thick composite sheet consisting of 12 layers of 0/90 fabric using vacuum infusion, which was coated with a 1 mm thick coating on its upper surface by casting. The post-cured composites were finally cut to dimensions of 100 mm x 100 mm x 4 mm for the cone calorimetry tests and 80 mm x 15 mm x 4 mm for the bending tests. All test specimens were crosslinked for 24 hours at room temperature and then post-crosslinked at 100 °C in two cycles, first for 2 hours and then for 1 hour.

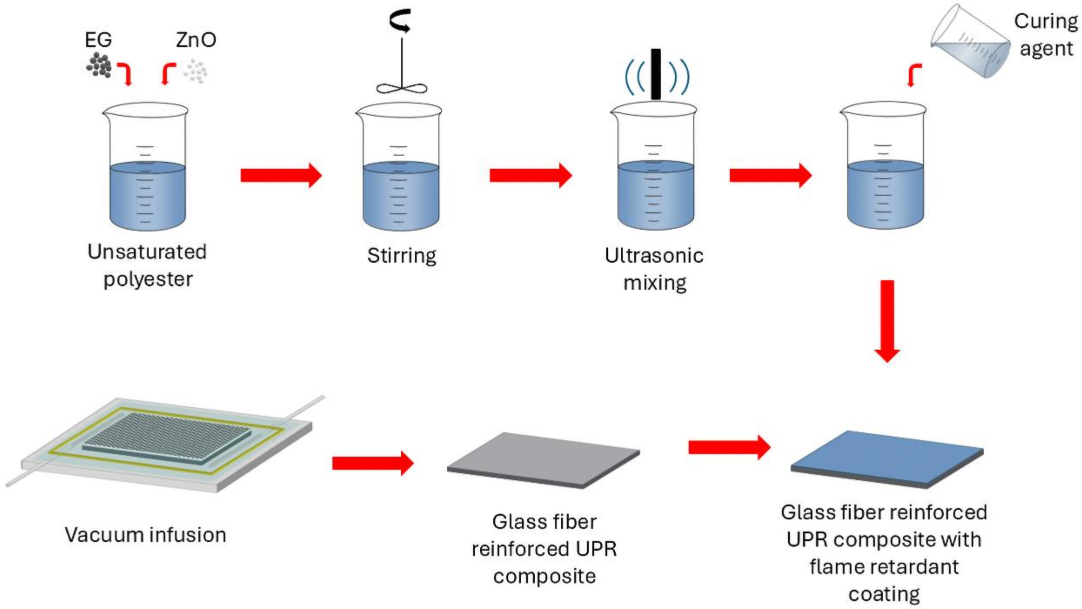

Figure 2: Preparation stages of the glass fiber reinforced UPR composites with flame retardant coating.

2.3. Testing and characterization

TGA

For the thermal stability test, we used a TA Instruments Q500 thermogravimetric analyzer (New Castle, DE, USA). The test was performed between 30 and 600 °C at a heating rate of 20 °C/min in a nitrogen atmosphere with a 30 ml/min flow rate. The samples weighed 5–10 mg, and the data were evaluated with the TA Universal Analysis program.

UL 94 tests

The UL 94 standard flammability test was performed in accordance with the ISO 9772 and ISO 9773 standards. In the horizontal arrangement (H-type), the 120x10x4 mm samples were exposed to a 30 s ignition, and after the flame was removed, the time taken for the flame front to advance between the 25 mm and 100 mm marks was measured. From this burning time , the flame spread rate was determined with formula (1):

$$v = 60 \cdot \frac{L}{t} \tag{1}$$

where v is the flame spread rate [mm/min], L is the burning distance between the two markings [mm], and t is the burning time between the two markings [min].

The flame retardancy rating of the samples was determined from the vertical (V-type) arrangement.

Glow wire flammability index (GWFI) test

The flammability of the coatings and coated composites was also characterized with the glow wire flammability index in accordance with IEC 60695. We used a T04-08 type device (Testing d. o. o., Slovenia), and the surface area of the tested samples was 60 mm x 60 mm. The thickness of the reference composite was 3 mm, while the thickness of the coated composites was 4 mm.

Cone calorimetry

The combustion properties of the coatings and coated composites were tested with a TCC 918 Cone Calorimeter (NETZSCH TAURUS Instruments GmbH, Germany) in accordance with ISO 5660-1. The test specimens had a surface area of 100 mm x 100 mm. The samples were exposed to 50 kW/m^2 radiant heat and ignited with a spark igniter. In addition to heat release, the amount of gases generated was also examined. The following parameters were determined from the cone calorimetric measurement: time to ignition (TTI), peak heat release rate (pHRR), time to pHRR (t_{pHRR}), total heat release (THR), total smoke production (TPS), maximal average rate of heat emission (MARHE), effective heat of combustion (EHC), residual mass, flame retardancy index (FRI), and the total emission of CO and CO_2. To determine the FRI value, equation (2) was used.

$$FRI = \frac{\left(\frac{THR \cdot pHRR}{TTI}\right)_{reference}}{\left(\frac{THR \cdot pHRR}{TTI}\right)_{modified}} \tag{2}$$

The Flame Retardancy Index (FRI) is a dimensionless indicator commonly employed to evaluate and compare the fire performance of flame-retarded polymers with that of their reference materials. According to the FRI value, polymers can be classified as having poor flame retardancy when FRI < 1, good flame retardancy when 1 < FRI < 10, and excellent flame retardancy when FRI > 10.

SEM-EDS

The structure and elemental distribution of the residues after combustion were examined by scanning electron microscopy (SEM-EDS) combined with energy dispersive spectrometry, with a JEOL JSM 6380LA (Jeol LTD., Tokyo, Japan) scanning electron microscope at 500x magnification. To avoid charging, we coated the samples with gold with a Jeol JPC1200 cathodic sputtering gold coating device (Jeol Ltd., Tokyo, Japan).

Porosity

The porosity of the coatings and coated composites was determined with a Sartorius Quintix precision balance (Sartorius, Göttingen, Germany). To calculate porosity, we determined the density from the weights measured in air at 25 °C and in distilled water, and compared it with the theoretical density derived from the composition. The surface area of the samples tested was 15 mm x 15 mm. We examined 3 samples of each composition.

The porosity of the reference and flame-retardant UPR samples was determined with equation (3), where the theoretical densities were calculated taking into account the amount of flame retardants [24]:

$$P_{coating} = 100 - \frac{\rho_{m,coating}}{\rho_{t,coating}} \cdot 100 \tag{3}$$

where $P_{coating}$ is the porosity [%] of the reference and flame-retardant UPR samples, $\rho_{m,coating}$ is the measured density of the reference or flame-retardant UPR coating [g/cm^3], $\rho_{t,coating}$ is the theoretical density of the reference or flame-retardant UPR coating [g/cm^3].

The fiber content of the glass fiber–reinforced UPR composite was calculated as 60%. Porosity was determined with equation (4), while the theoretical density of the composite was calculated with equation (5) [24]:

$$P_{composite} = 100 - \frac{\rho_{m,composite}}{\rho_{t,composite}} \cdot 100 \tag{4}$$

$$\rho_{t,composite} = \frac{1}{\frac{0,4}{\rho_{t,matrix}} + \frac{0,6}{\rho_{t,fiber}}} \tag{5}$$

where $P_{composite}$ is the porosity of the UPR composite [%], $\rho_{m,composite}$ is the measured density of the composite [g/cm^3], $\rho_{t,composite}$ is the theoretical density of the composite [g/cm^3], $\rho_{t,matrix}$ is the theoretical density of the UPR matrix [g/cm^3], $\rho_{t,fiber}$ is the theoretical density of the reinforcement [g/cm^3].

To determine the porosity of coated composites, we used the ratio of the thickness of the composite to the thickness of the coating.

$$P_{cc} = 100 - \frac{\rho_{m,cc}}{\rho_{t,cc}} \cdot 100 \tag{6}$$

$$\rho_{t,cc} = \frac{3}{3+1} \cdot \rho_{t,composite} + \frac{1}{3+1} \cdot \rho_{t,coating} \tag{7}$$

where P_{cc} is the porosity of the coated composite [%], $\rho_{m,cc}$ is the measured density of the coated composite [g/cm^3], and $\rho_{t,cc}$ is the theoretical density of the coated composite [g/cm^3].

Hardness tests

The Shore D hardness of the coatings and coated composites was determined with a Zwick H04.3150.000 hardness tester (Zwick GmbH & Co. KG, Ulm, Germany) according to ISO 48-2:2018. The test was performed on 4 mm thick samples with a load of 50 N. Indentation time was 3 s, and 10 measurement points were recorded on each sample.

Pull-off test

The adhesion between the coating and the composite was tested with a pull-off adhesion test based on ISO 4624:2016. A DeFelsko PosiTest AT-M device (DeFelsko, New York, USA) was used for the test. The diameter of the dollies, which were cleaned with methanol before the test, was 20 mm. Circular coatings with a diameter of 20 mm were created on the surface of the composite. The dollies were attached to the coating with the Araldite 2011 two-component adhesive and left to crosslink for 24 hours. During the test, with the use of the diameter of the dollies, the device gives the pull-off strength between the composite and the coating in MPa. We performed 6 tests per composition.

Bending tests

Bending tests were performed on a Zwick Z005 tensile testing machine (Zwick GmbH & Co. KG, Germany). Bending strength was determined in accordance with ISO 14125, on 80 mm x 10 mm x 4 mm test specimens in three-point configuration with a support length of 64 mm and a speed of 2 mm/min. Five tests were performed for each setup.

3. Results and discussion

3.1. Thermal and flammability properties

3.1.1. Thermogravimetric Analysis

The thermal stability of the additives itself and the coatings was examined by TGA. The results are summarized in Figure 3 and Table 3.

Table 3: TGA results for the coatings examined

Sample name	$T_{-5\%}$ [°C]	$T_{-50\%}$ [°C]	dTG_{max} [%/°C]	T_{dTGmax} [°C]	Residual mass at 600 °C [%]
EG	228	-	0.43	228	75.7
UPR	292	393	1.28	409	5.5
UPR/ZnO	292	400	0.63	385	30.0
UPR/EG	286	339	4.55	296	5.1
UPR/ZnO/EG	286	391	0.74	389	27.5

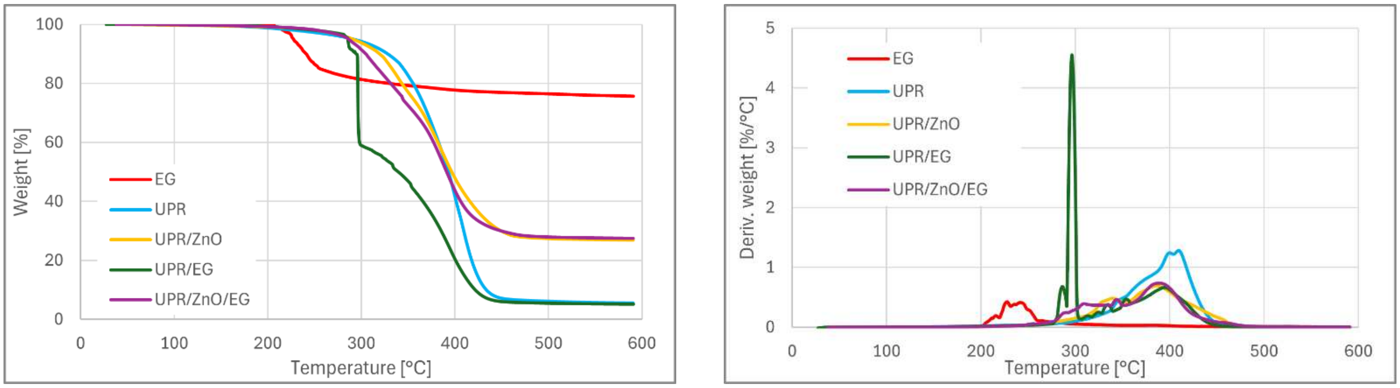

a) b)

Figure 3: TGA (a) and derivative thermogravimetric (DTG) (b) curves of the coatings examined

The temperature at 5% mass loss ($T_{-5\%}$) in the reference sample without additives was 292 °C. ZnO did not change $T_{-5\%}$, but it decreased under the influence of EG. This reduction can be explained by the fact that expandable graphite begins to expand at a lower temperature (220 °C). The $T_{-5\%}$ of the mixed composition was also 286 °C, so the presence of ZnO did not decrease the initial decomposition temperature compared to the samples containing EG.

ZnO increased the temperature of 50% mass loss ($T_{-50\%}$) compared to the reference, because ZnO decomposes only at high temperatures, thus shifting the mass loss to higher temperatures. EG significantly reduced $T_{-50\%}$, because it expands at lower temperatures. However, adding ZnO improves thermal stability and shifts $T_{-50\%}$ towards higher temperatures, making it almost identical to the reference temperature, 393°C.

The maximum mass loss rate (d_{TGmax}) of the reference was 1.28%/°C, which was reduced to 0.63%/°C by ZnO. However, d_{TGmax} increased significantly for expandable graphite. Figure 3b) shows that the sample containing EG showed a sudden mass loss at 296 °C. The explanation for this is the expansion of EG, which causes gases generated during volume expansion to escape from the matrix, resulting in a sudden mass loss on the curve. This may also affect d_{TGmax}. In the case of the mixed composition, we did not observe such a sudden decrease in mass.

The highest temperature corresponding to the maximum mass loss rate (T_{dTGmax}) was observed in the case of the reference (409 °C). The samples containing ZnO only and ZnO and EG reduced T_{dTGmax} by nearly 20 °C. The lowest T_{dTGmax} was found in the sample containing only EG (296 °C).

3.1.2. UL 94 flammability test

The results of the UL 94 flammability test of the coatings are shown in Table 4. We did not perform tests on the composites because the coating is applied only on one surface of the composite, so we would not obtain representative results with this type of test. Figure 4 shows the behavior of different samples in the test.

Table 4: The results of the UL 94 flammability tests

Sample name	Horizontal test		Vertical test				
	Completed the horizontal test?	Flame spread rate (mm/min)	Cotton wool was ignited?	Did it burn up completely?	Smoldering flame?	Spark formation during combustion	Classification
UPR	**no**	**20**	**-**	**-**	**significant**	**no**	**HB/20**
UPR/ZnO	**no**	**26**	**-**	**-**	**moderate**	**no**	**HB/26**
UPR/EG	**yes**	**-**	**no**	**yes**	**weak**	**yes**	**HB**
UPR/ZnO/EG	**yes**	**-**	**yes**	**yes**	**none**	**yes**	**HB**

The reference UPR samples and the samples containing ZnO had an HB rating in the horizontal test. The flame spread rate increased to 26.10 mm/min with the addition of ZnO, but the flame was less sooty because of the flame retardant effect, which is due to the carbon-forming properties of ZnO, as ZnO aids the carbonization process, promoting the formation of a heat-insulating carbon layer that inhibits the release of flammable gases and thus also reduces soot formation. This property promoted faster flame spread, but moderated smoke and soot formation. In the case of samples containing EG, and both EG and ZnO, we observed that the flame went out before the first signal in the horizontal test, due to the formation of a heat-insulating graphite layer during the expansion of EG, which formed a physical barrier that inhibited combustion and prevented its further spread. During the vertical test, we observed significant sparking in both compositions due to the expansion of EG. The samples exhibited a sparkler-like phenomenon during burning, and glowing particles detached and fell. However, in the case of the sample containing EG, the cotton wool placed underneath did not ignite, i.e., the combustion was well localized, as the EG layer acted as a heat insulator. Despite the glowing particles, it did not generate enough heat to ignite the cotton wool underneath.

In the case of the mixed composition, the combination of the two additives resulted in a more balanced effect. ZnO further reduced soot formation. The synergistic effect of ZnO and EG promoted the formation of a stable, non-combustible layer, which further limited combustion processes by reducing heat and oxygen access. However, in the mixed samples, the cotton wool placed under the sample ignited because ZnO held together the resulting carbonized layer, which absorbed a sufficient amount of heat, and the expansion of EG caused particles to fall. The dripping pieces reached the ignition temperature, unlike the sample containing only EG, and ignited the cotton wool. In the vertical test, all samples burned until they were clamped, so the samples were given an HB rating.

a) b) c) d)

Figure 4: UL 94 tests: a) UPR, b) UPR/ZnO, c) UPR/EG, d) UPR/ZnO/EG

3.1.3. GWFI test

The flammability properties of coated composites and the effectiveness of coatings were tested with a glow-wire flammability index (GWFI) test. GWFI expresses the highest temperature at which the material extinguishes within 30 seconds after being in contact with the glowing wire for 30 seconds. The UPR/GF+UPR_ctg sample ignited in 7 seconds at 700 °C, burned with a flame 3–4 cm high, and the glow wire penetration depth was 4 mm. The sample continued to burn for more than 30 seconds after the test, so we continued the test at 650 °C. At that temperature, the sample did not ignite, only heated the coating and smoked, and the glow wire reached a penetration depth of 2 mm. The UPR/GF+UPR_ctg sample received a rating of 650/4. In the rating, the first number indicates the highest temperature that complies with GWFI specifications, and the number after the "/" indicates the thickness of the sample. Since the pure UPR-based coating did not contain any effective flame retardant additives, it was able to ignite even at relatively low temperatures and burn for a long time. The high penetration depth and sustained burning were due to the low thermal stability of the coating and the formation of gases during combustion. The UPR/GF+ZnO_ctg sample ignited at a higher temperature. At 800 °C, it burned with a 3 cm high flame, its ignition time was 3 s, and the glowing wire penetrated 1 mm into the coating. At 750 °C, the sample did not ignite, only smoked, with the glowing wire penetrating 1 mm. The UPR/GF+ZnO_ctg sample had a rating of 750/4. This is because ZnO improved the thermal stability of the coating and reduced the amount of combustible gases produced during combustion, which was examined during cone calorimetry. Since ZnO was present in the coating as an inorganic component, it increased the GWFI of the coating, as it only ignited at a temperature 100 °C higher. The UPR/GF+EG_ctg sample ignited in 2–3 seconds at 960 °C, burned with a 7 cm high flame, and the incandescent filament penetrated 2 mm into the coating. During combustion, a 1.5–1.9 mm carbon foam formed around the ignition site. However, when the glowing wire was removed, the sample was immediately extinguished, so the rating of the UPR/GF+EG_ctg sample was 960/4. The expansion of EG due to combustion created a physical barrier between the oxygen and combustible components, reducing the chance and intensity of continued combustion. The carbon foam also conducted the heat away from the polymer due to its thermal conductivity, further hindering the continuation of combustion. The immediate extinguishing of the sample after the removal of the glowing wire was due to the properties of EG, as it was structurally unstable and disintegrated when the glowing wire was removed. The UPR/GF+ZnO/EG_ctg sample ignited at 960 °C within 1–2 seconds and burned with a flame height of 3 cm, with the glowing wire penetrating 1 mm into the coating. During combustion, a 2.4–2.6 mm thick carbon foam formed. After removing the glowing wire, the sample was extinguished within 5–6 seconds, thus the UPR/GF+ZnO/EG_ctg sample was classified as 960/4. The combined use of ZnO and EG showed a synergistic effect. EG primarily formed a physical barrier through its expansion, while ZnO chemically promoted the degree of carbonization and the stability of its structure. Figure 5 shows the GWFI samples after the test. All of the images show heavy discolorations. There were burn marks on samples containing EG, and worm-like formations that had formed during the expansion of EG fell off the burnt surface, thus reducing the functionality of the coating. This eliminates the thermal protection provided by the carbon foam, and the layer underneath becomes flammable again. When EG and ZnO were used together, the carbon foam that formed remained on the heated surface, providing a durable thermal protection layer and functioning as a protective char layer that limited heat and oxygen transfer, thereby increasing the flame retardancy of the material. The presence of ZnO helped to stabilize the carbonization process and maintain the structural stability of the foam structure.

a) b) c) d)

Figure 5: GWFI samples after the test:
a) UPR/GF+UPR_ctg, b) UPR/GF+ZnO_ctg, c) UPR/GF+EG_ctg, d) UPR/GF+EG/ZnO_ctg

3.1.4. Cone calorimetry

Table 5 shows the results of cone calorimetry.

Table 5: Cone calorimetry results

Sample	**TTI**	**pHRR**	t_{pHRR}	**THR**	**TSP**	COY	CO_2Y	CO/CO_2	**MARHE**	**EHC**	**FRI**	**Residual mass**
	[s]	**[kW/m²]**	**[s]**	**[MJ/m²]**	**[m²/m²]**	[g/g]	[g/g]	[-]	**[kW/m²]**	**[MJ/kg]**	**[-]**	**[%]**
UPR	38	783	222	107.3	6073	0.07	1.77	0.039	465	3156	-	0.74
UPR/ZnO	35	726	130	124.0	4333	0.04	1.83	0.021	648	70	0.86	31.67
UPR/EG	19	262	90	125.2	4408	0.04	1.88	0.024	198	401	1.28	5.89
UPR/ZnO/EG	34	303	173	78.8	1737	0.03	1.64	0.021	167	41	3.15	37.56
UPR/GF+UPR_ctg	44	485	133	69.0	3632	0.05	1.59	0.033	238	19	-	52.49
UPR/GF+ZnO_ctg	42	517	125	87.5	3875	0.04	1.78	0.020	243	19	0.71	55.80
UPR/GF+EG_ctg	31	324	103	73.1	3397	0.05	1.76	0.028	154	19	0.99	54.79

UPR/GF+EG/ZnO_ctg	33	317	102	78.3	2196	0.03	1.84	0.014	131	18	1.01	58.99

During the test, we examined the coatings on their own and on the surface of the composites. In the case of coatings (without composites), the time to ignition (TTI) of the reference UPR sample was 38 s, but the coatings containing flame retardants ignited sooner. The lowest ignition time (19 s) was observed in the sample containing only EG, which can be explained by the fact that EG begins to act at lower temperatures, in good correlation with the TGA results shown in Table 3.

The peak heat release rate (pHRR) decreased in all cases compared to the reference sample. However, the time to pHRR (t_{pHRR}) was lower than the reference value (222 s) for all flame retardants. The heat release curves (Figure 6) show that the reference sample is characterized by an intense and narrow peak, which shows that the sample burns completely in a short time after a sudden heat release. The heat release curve of the sample containing only ZnO is not as narrow, while the sample containing EG has a gradually declining curve. This is typical of condensed-phase flame retardants, as heat release gradually decreases after the charred protective layer forms. In the mixed sample, both the more intense peak characteristic of ZnO and the decay characteristic of EG can be observed.

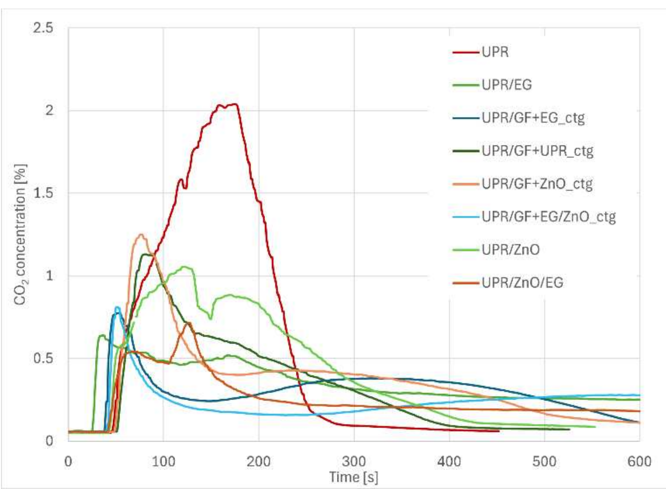

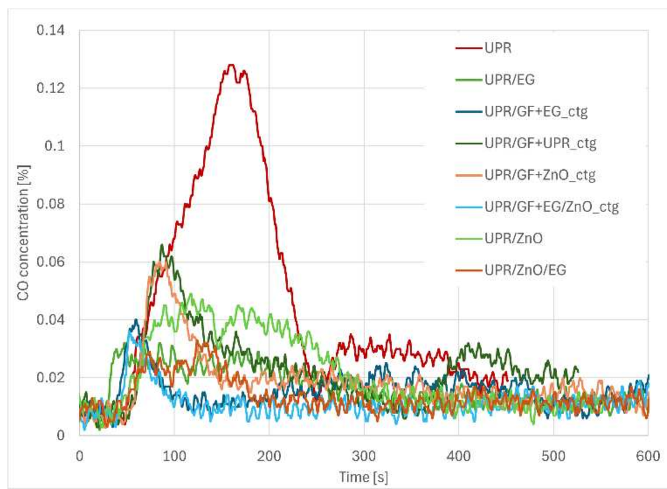

a)

b)

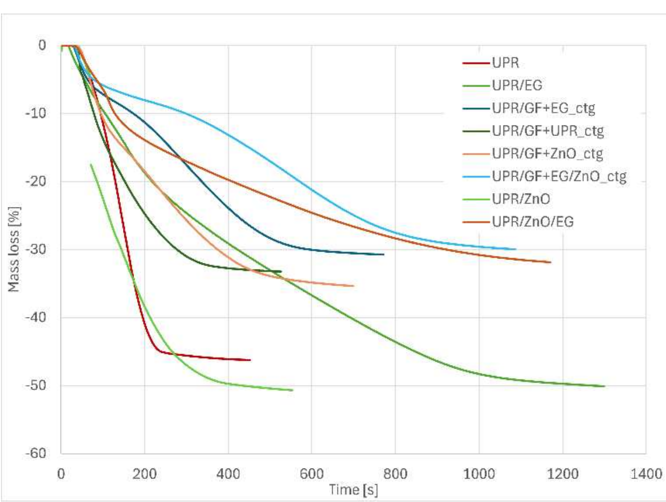

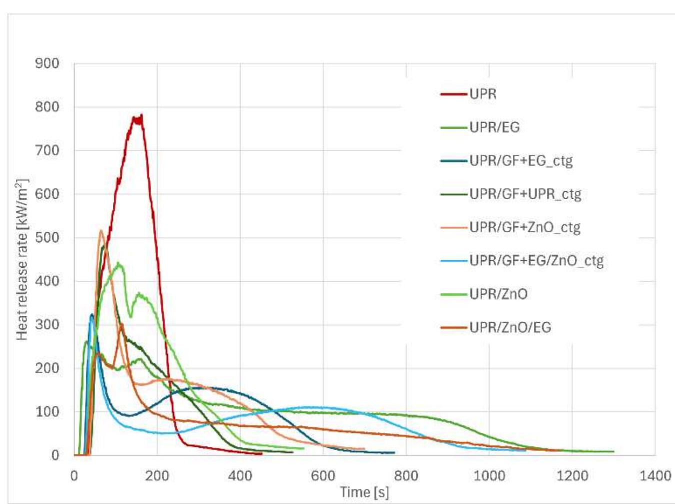

c) d)

Figure 6: Cone calorimetry curves: a) CO_2 emission curves, b) CO emission curves, c) mass reduction curves, d) heat release rate curves

Total heat release (THR) decreased compared to the reference only in the case of the mixed composition. However, a significant decrease in total smoke production (TSP) was observed for all flame retardants, with the lowest value produced by the mixed composition, which was 71% lower than the reference value. The maximum average rate of heat emission (MARHE) decreased compared to the reference UPR, except for the UPR/ZnO sample, while the effective heat of combustion (EHC) was lower in all the flame-retarded samples. The two flame retardants together significantly reduced both MARHE and EHC values, from which we can conclude that flame retardants mainly act in the condensed phase. The FRI value of the coating containing only ZnO is 0.86, indicating poor fire retardancy. In the case of EG, this value increased to 1.28, while in the case of the mixed composition, it was 3.15, which can be considered a good flame retardancy.

The reference sample burned almost entirely during the test, with only 0.74% of the mass remaining. The residual mass increased due to the effect of the flame retardants, and in the case of the mixed composition, 37.56% of the sample remained after burning. The increase in residual mass also suggests a condensed phase mechanism. Figure 6 a) and b) show that carbon dioxide (CO_2) and carbon monoxide (CO) emissions of the reference sample were intense, but decreased considerably due to the flame retardants.

EG and ZnO individually and together reduced CO yield (COY) and the CO/CO_2 ratio, indicating more complete oxidation and less gas from incomplete combustion. In the UPR/EG sample, CO_2 yield (CO_2Y) increased and COY decreased, as well as the CO/CO_2 ratio. Therefore, it can be concluded that EG promoted more complete oxidation and that the protective layer inhibited soot and smoke formation. UPR/ZnO also increased CO_2Y but decreased COY and the CO/CO_2 ratio, suggesting that it promotes condensed-phase carbonization. The combined flame retardants had the lowest COY, suggesting that the condensed-phase protective layer effectively reduced the release of combustible gases and smoke formation.The TTI of the coated composites showed a similar trend to the coatings. All flame-retardant samples ignited earlier than the reference. Only the UPR/GF+ZnO_ctg sample did not reduce the pHRR, but the composites with EG, and EG and ZnO produced a significant reduction. Similar to coatings, the peak heat release occurred earlier in coated composites, and the THR also increased compared to the reference. The heat release curves show that a second peak began to form after the heat release decreased in the case of coatings containing flame retardants. This second peak is due to the fact that after the coating burned, the fire reached the composite matrix, causing the heat release to increase again.

TSP decreased compared to the reference (3632 m^2/m^2), except for the UPR/GF+EG/ZnO_ctg sample, and the mixed sample had the lowest TSP, 2196 m^2/m^2. The maximum average heat release rate was similar. The UPR/GF/ZnO sample slightly increased the maximum average rate of heat emission, but EG, and EG and ZnO together decreased it. The EHC decreased only with the mixed composition, while the residual mass increased in all samples containing flame retardants compared to the reference UPR/GF/UPR sample. The trend in the FRI values of coated composites is similar to that of coatings. The lowest FRI value is for the UPR/GF+ZnO_ctg sample, and the highest (1.01) is for the coated composite containing a mixed composition.

In coated UPR/GF composites, coatings with ZnO and EG reduce COY and the CO/CO_2 ratio compared to pure UPR coating, suggesting a condensed-phase mechanism and more complete oxidation. The effects of EG and ZnO, both individually and in combination, increased CO_2 yield, indicating that the carbon layer formed by the coating promotes more complete oxidation. The mixed composition sample had the lowest CO yield and CO/CO_2 ratio, suggesting that the stable, thick carbon layer formed on the composite surface most effectively limits smoke formation and the formation of partly oxidized combustion products.

Overall, mixed coatings significantly reduce the pHRR, TSP, MARHE, and EHC, while increasing residual mass. However, they reduce the time to ignition and increase the THR.

3.1.5. Analysis of residues after combustion

Figure 7 shows the combustion residues of the reference UPR sample and coatings remaining after the cone calorimetry tests. In the case of pure UPR, the 0.74% sample mass remaining in the cone calorimetry test consisted only of soot/carbon residues. The samples containing ZnO had a stable structure, but ZnO enrichment was observed in the upper layers, while the lower layers consisted only of blackened combustion residues. In the sample containing only EG, there were worm-like formations characteristic of EG. Samples containing both ZnO and EG showed the combined effect of the two additives.

a) b) c) d)

Figure 7: Structures remaining after cone calorimetry: a) UPR, b) UPR/ZnO, c) UPR/EG, d) UPR/ZnO/EG

Figure 8 shows SEM images of the combustion residues at 100x magnification. Figure 8a shows the residue without flame retardant. Figure 8b shows samples containing only EG, where the characteristic worm shape is clearly visible. Figure 8c shows a sample containing only ZnO, showing a thick layer of ZnO, which is closed and only has cracks due to thermal expansion, as well as a few holes/gaps where the internal gases escaped. Figure 8d shows an SEM image of a sample containing both ZnO and EG, where the worm-like characteristics of EG are also visible, but they are held together by ZnO intercalations and clusters, which is consistent with the effect of ZnO observed in the UL 94 tests.

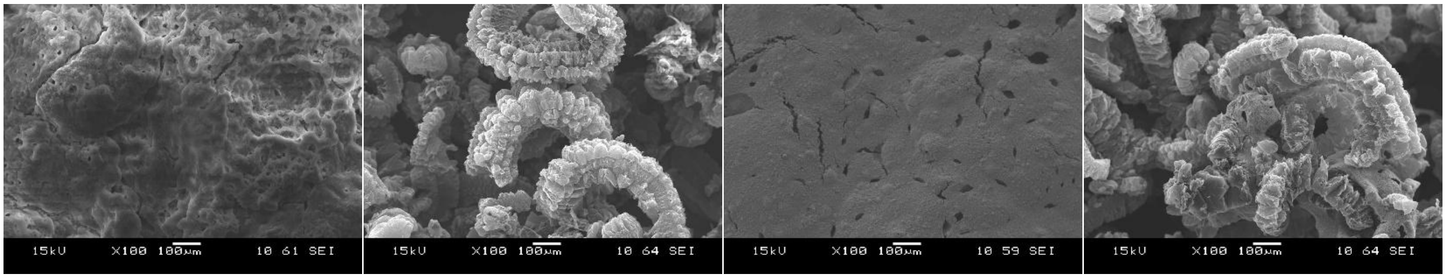

a) b) c) d)

Figure 8: SEM images after combustion:
a) UPR combustion residue, b) UPR/ZnO combustion residue, c) UPR/EG combustion residue, d) UPR/ZnO/EG combustion residue

The SEM-EDS tests show that the sample without flame retardant consisted only of carbon and oxygen, as well as aluminum from the tray used during the test. However, due to its small amount, we were unable to perform a representative analysis on the remaining combustion residue. In the coating containing only ZnO, the top layer contained 2.30 m/m% carbon, 14.75 m/m% oxygen, and 82.95 m/m% zinc. The bottom layer of the combustion residue contained 24.66 m/m% carbon, 15.39 m/m% oxygen, and 59.95 m/m% zinc. This can be explained by the fact that ZnO accumulated in the upper layer during combustion, because ZnO is thermally stable and, as an inorganic oxide, cannot decompose in the temperature range studied, unlike the organic matrix, which decomposed and burned as a result of heat. The combustion and decomposition of the matrix material increased the relative concentration of ZnO, especially in the surface zone, where the intensity of combustion was highest. Furthermore, ZnO particles also migrated towards the surface through the heat-induced gas flows and the already burned, porous matrix, which further increased their concentration [25] (Figure 9).

The combustion residue of the sample containing only EG consisted of 89.08 m/m% carbon and 10.92 m/m% oxygen. The top layer of the coating containing both ZnO and EG had a combustion residue of 54.6 m/m% carbon, 9.17 m/m% oxygen, and 36.23 m/m% zinc. The bottom layer of the combustion residue contained 89.17 m/m% carbon, 8.185 m/m% oxygen, and 2.645 m/m% zinc. Here, too, there was a zinc enrichment in the upper layers of the coating containing only ZnO, but here the combustion residue had different proportions due to the high proportion of excess carbon from the EG.

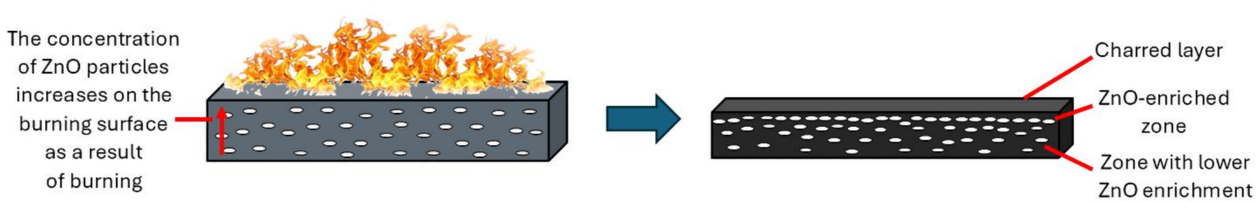

Figure 9: The process of char formation

3.2. Structural properties

3.2.1. Porosity tests

Figure 10 shows the results of the porosity testing of the coatings and the composite reference and coated composites.

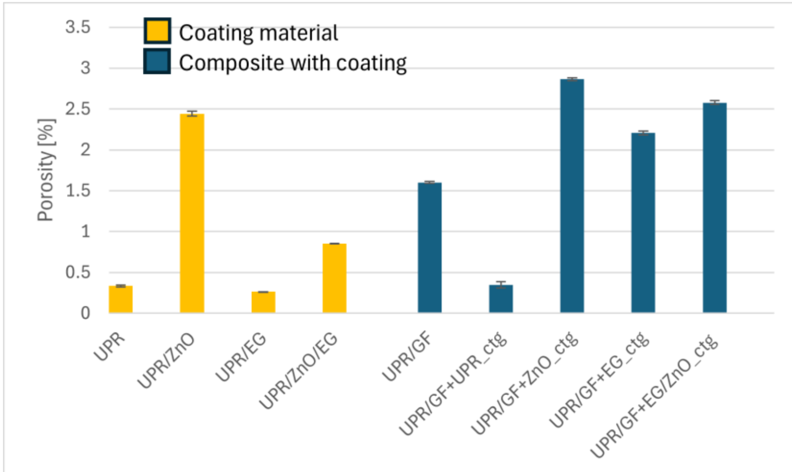

Figure 10: The porosity of coatings and of coated composites

The porosity of the UPR sample was 0.3%, which did not change significantly due to the effect of expandable graphite. In contrast, ZnO increased porosity to 2.4%. The reason for this is that expandable graphite has a lamellar structure, so it does not significantly affect the flow of resin. In contrast, ZnO has an amorphous structure, which allows air bubbles to remain between its particles. Furthermore, unmodified nanoscale ZnO particles tend to aggregate, which makes the surface of the UPR matrix uneven. Another problem may have been that the difference between the shrinkage rate of the ZnO aggregates and the UPR resin resulted in microcracks on the surface of the sample [26]. With a mixed composition, we had higher porosity compared to the reference, and adding EG reduced porosity compared to the sample containing only ZnO.

The porosity of the glass fiber–reinforced reference composite was 1.6%, which is significantly higher than that of the UPR sample. This can be explained by the more air bubbles forming between the reinforcing materials. The UPR_ctg sample had the lowest porosity of the coated composites at 0.3%. Since the coating did not contain additives, the resin flowed more easily into the microcracks formed in the composite, reducing porosity. For composites with coatings containing additives, results similar to those for pure UPR coatings can be observed. The highest porosity was observed in the case of ZnO, which can be reduced by adding EG. The coating containing only EG has lower porosity than the coating containing only ZnO or the mixed composition.

3.2.2. Hardness measurement

Figure 11 shows the results of Shore D hardness tests for coatings and coated composites.

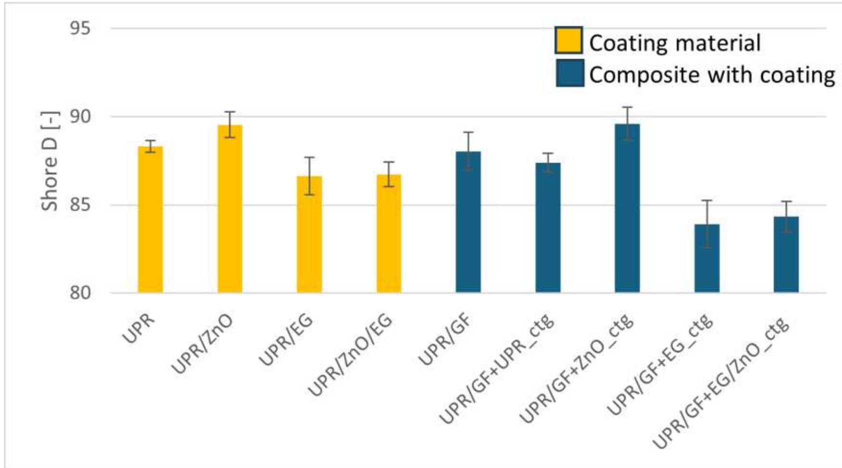

Figure 11: Shore D hardness of coatings and coated composites

The hardness of the reference UPR coating was 88 Shore D, consistent with literature data [27]. The additives slightly modified the hardness. The effect of ZnO increased the hardness, which can be explained by its stiffening effect. EG slightly decreased hardness (86 Shore D), which can be explained by the layered, porous structure of the EG particles and the poorer adhesion between the UPR matrix and EG. The solid but mechanically deformable graphite sheets of EG do not participate effectively in load transfer, thereby reducing the macroscopic hardness of the material. Furthermore, EG can create local micropores in the matrix, which impairs its structural integrity and contributes to a slight deterioration of mechanical properties, such as hardness [28]. In the case of mixed compositions, ZnO did not significantly change hardness compared to the sample containing only EG.

The trend is similar in coated composites. The hardness of the uncoated reference was also 88 Shore D. The UPR coating without additives reduced this to 87 Shore D, while ZnO increased it to 89 Shore D. The sample containing only EG had the lowest hardness, which slightly increased when ZnO was added.

3.2.3. Adhesion and bending tests

In the case of coated composites, it is important to determine the adhesion between the surface of the composite and the coating. We used a pull-off test to examine this. For coated composites, peel strength was nearly equal in all cases, at around 2 MPa. The reason for this is that in all cases, it was not the coating that peeled off, but rather the top matrix layer of the composite. This indicates cohesive failure in the samples. To obtain more accurate adhesion results, we performed three-point bending tests.

During the three-point bending tests, we examined the test specimens in two different arrangements. In one case, the coatings were on the compressed side, where we tested for possible external impact on the composite product. In the other case, they were located on the tensile side of the test specimen. The results of the three-point bending tests are shown in Table 6.

Table 6: Results of bending tests.

Sample name	Flexural strength [MPa]	Modulus of elasticity [GPa]	Deflection at failure [mm]	Deflection when the first crack appeared [mm]	Coating location
UPR/GF	486.0	65.8	5.6	-	**-**
UPR/GF+UPR_ctg	379.0	48.8	5.4	-	**Compression side**
UPR/GF+ZnO_ctg	366.9	46.9	5.6	-	
UPR/GF+EG_ctg	382.7	52.4	5.1	-	
UPR/GF+EG/ZnO_ctg	352.4	51.2	4.5	-	
UPR/GF+UPR_ctg	343.3	60.6	4.9	2.6	**Tension side**
UPR/GF+ZnO_ctg	317.9	57.0	5.5	1.5	
UPR/GF+EG_ctg	393.4	67.6	5.2	1.3	
UPR/GF+EG/ZnO_ctg	332.0	60.8	5.1	1.0	

The uncoated reference, the UPR/GF sample, had a flexural strength of 486.0 MPa, a flexural modulus of 65.8 GPa, and failed at a deflection of 5.6 mm. In both compression-type and tension-type tests, all coated composites had lower flexural strength and deflection at failure than the reference. This is because the interface layer between the matrix and the coating layer can be considered the weakest point of the system, leading to the localization of failure. This is confirmed by the fact that failure occurred in the matrix–coating interface layer in both compression-type and tension-type tests. The most significant difference between the two-sided tests was in the mode of failure. Figure 12 shows the test curves for the different failure modes on the two sides. In the case of compression-type tests, failure occurred in the adhesion boundary layer between the coating and the composite in each test, with the coating remaining structurally intact on the composite. In the case of tensile-type tests, the coating cracked at a given deflection level at the point of most significant deformation (in the middle of the sample), parallel to the width of the test specimen, initiating failure. At the point of final failure, further cracks appeared, resulting in the fragmentation of the coating.

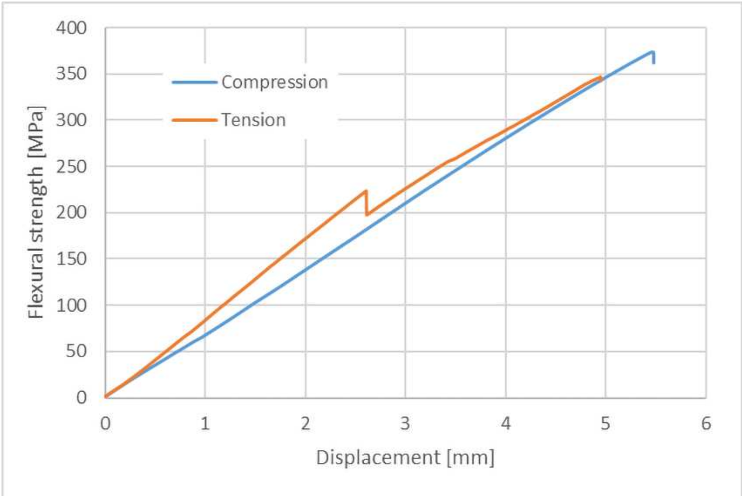

Figure 1: Typical bending curves for compression-type and tensile-type sides

Compared to samples coated only with UPR, the EG-coated sample exhibited higher flexural strength (382.7 MPa and 393.4 MPa) and modulus on both the compressed and tensile sides, which was due to the layered and porous structure of EG. EG contributed to more efficient load distribution and internal stress absorption, which increased the load-bearing capacity and stiffness of the entire structure. However, EG is less resistant at the microstructural level due to its structure, so the samples reached failure deflections sooner. Compared to samples coated with UPR alone, ZnO slightly reduced the flexural strength and modulus of the sample on both the compressed and tensile sides. This can be explained by the brittle, ceramic properties of ZnO, which made it less effective at distributing the load. However, thanks to its more homogeneous, crystalline structure, ZnO was more resistant to forming primary microcracks, thus increasing deflection associated with failure. When EG and ZnO were used together, the strength of the samples remained lower than the flexural strength and modulus of samples with coatings containing only EG, and the failure values were also lower than when the two additives were used. This is because the combined use of EG and ZnO resulted in coatings with a higher degree of filling, which were more brittle and prone to cracking. Also, the first cracks appeared on the tensile side at the lowest deflection when EG and ZnO were used together. However, although the cracks appeared early, only the coatings applied in combination remained intact during the tensile side tests but when EG and ZnO were not used together, they typically flaked off during final failure. This property is advantageous, as in this case, the coating can remain on the surface of the composite even when the composite–coating boundary fails.

4. Conclusions

Multifunctional halogen-free coatings containing zinc oxide (ZnO) and expandable graphite (EG) effectively enhanced the fire and mechanical performance of glass fibre–reinforced unsaturated polyester (UPR) composites.

For the coated composites, the combined use of ZnO and EG resulted in an 34% (from 485 kW/m^2 to 317 kW/m^2) reduction in the peak heat release rate (pHRR) and a 44% decrease (from 238 kW/m^2 to 131 kW/m^2) in the maximum average rate of heat emission (MARHE) compared to the pure UPR coating. Total smoke formation was reduced by more than 70%. In glow wire flammability index tests, the ignition index increased from 650 °C for the reference composite to 750 °C with ZnO, and to 960 °C with EG or with the combined ZnO–EG coating.

The synergistic effect between ZnO and EG generated a stable, cohesive intumescent char layer that acted as a physical barrier, limiting heat and oxygen transfer. During combustion, ZnO promoted char formation and crosslinking within the carbonaceous residue, effectively binding the expanded graphite structure. This mechanism led to more controlled combustion, reduced heat release, and enhanced flame retardancy of the coated composites.

Mechanical testing indicated that the additives did not influence the adhesion, while the ZnO–EG combination showed improved toughness and superior crack dispersion under bending stress. The dense particle network helped distribute microcracks, allowing the coating to retain its integrity and adhesion even under deformation.

In summary, the combined application of ZnO and EG is advantageous, as their synergistic interaction enhanced the flexural performance relative to their individual use, and simultaneously improved the outcomes in the UL-94, cone calorimetry, and GWFI tests. Such coatings are promising for use in applications in the future requiring both structural strength and flame retardancy, such as electrical panels, vehicle components, and composite panels in the construction industry.

Acknowledgements

The research reported in this paper was supported by the National Research, Development, and Innovation Office (NRDI, Hungary) through grants OTKA K 146236, OTKA K 138472 and OTKA K 142517. Project no. TKP-6-6/PALY-2021 has been implemented with the support provided by the Ministry of Culture and Innovation of Hungary from the National Research, Development and Innovation Fund, financed under the TKP2021-NVA funding scheme. The project 2022-2.1.1-NL-2022-00012 has been implemented with the support provided by the Ministry of Culture and Innovation of Hungary from the National Research, Development and Innovation Fund, financed under the 2022-2.1.1-NL Creation of National Laboratories, Complex Development funding scheme. Péter Csvila expresses appreciation for the support of the Doctoral Excellence Fellowship Programme (DCEP) funded by the National Research Development and Innovation Fund of the Ministry of Culture and Innovation and the Budapest University of Technology and Economics, under a grant agreement with the National Research, Development and Innovation Office.

References

[1] Á. Pomázi, M. Krecz, A. Toldy, “The effect of the combined application of solid- and gas-phase flame retardants in epoxy gelcoats on the thermal stability, fire performance and adhesion of coated carbon fibre–reinforced epoxy composites,” Journal of Thermal Analysis and Calorimetry 148 (2023): 257–270, https://doi.org/10.1007/s10973-022-11770-1.

[2] Z.J. Gombos, J. Summerscales, “In-mould gel-coating for polymer composites,” Composites Part A: Applied Science and Manufacturing 91 (2016): 203–210, https://doi.org/10.1016/j.compositesa.2016.10.014.

[3] G.S. Sudha, K.V. Arun, “Mechanical behaviour of gel coated laminated jute-epoxy composites under varied acidic media and loads,” Materials Today: Proceedings 27 (2020): 2953–2957, https://doi.org/10.1016/j.matpr.2020.03.838.

[4] L. Liu, Y. Xu, M. Xu, Y. He, S. Li, B. Li, “An efficient synergistic system for simultaneously enhancing the fire retardancy, moisture resistance and electrical insulation performance of unsaturated polyester resins,” Materials & Design 187 (2020): 108302, https://doi.org/10.1016/j.matdes.2019.108302.

[5] B. Mortaigne, S. Bourbigot, M. Le Bras, G. Cordellier, A. Baudry, J. Dufay, “Fire behaviour related to the thermal degradation of unsaturated polyesters,” Polymer Degradation and Stability 64 (1999): 443–448, https://doi.org/10.1016/S0141-3910(98)00149-9.

[6] A. Dowbysz, M. Samsonowicz, B. Kukfisz, P. Koperniak, “Recent Developments of Nano Flame Retardants for Unsaturated Polyester Resin,” Materials 17 (2024): 852, https://doi.org/10.3390/ma17040852.

[7] M.S. Murad, A.K. Hamzat, E. Asmatulu, R. Asmatulu, “Flame-retardant fiber composites: synergistic effects of additives on mechanical, thermal, chemical, and structural properties,” Advanced Composites and Hybrid Materials 8 (2024): 31, https://doi.org/10.1007/s42114-024-01111-1.

[8] European Chemicals Agency, “Regulatory strategy for flame retardants,” Publications Office of the European Union, LU, 2023, https://data.europa.eu/doi/10.2823/854233.

[9] T.R. Hull, A. Witkowski, L. Hollingbery, “Fire retardant action of mineral fillers,” Polymer Degradation and Stability 96 (2011): 1462–1469, https://doi.org/10.1016/j.polymdegradstab.2011.05.006.

[10] L.-L. Jiao, P.-C. Zhao, Z.-Q. Liu, Q.-S. Wu, D.-Q. Yan, Y.-L. Li, Y.-N. Chen, J.-S. Li, “Preparation of Magnesium Hydroxide Flame Retardant from Hydromagnesite and Enhance the Flame Retardant Performance of EVA,” Polymers 14 (2022): 1567, https://doi.org/10.3390/polym14081567.

[11] X. Zhai, Q. Ma, J. Lu, Y. Jin, R. Zhang, F. Luo, “Enhanced thermal stability and flame retardancy of PLA through intumescent flame retardant with B-modified ZSM-5 as a synergistic agent,” Express Polymer Letters 18 (2024): 326–336, https://doi.org/10.3144/expresspolymlett.2024.23.

[12] B. Mazela, A. Batista, W. Grześkowiak, “Expandable Graphite as a Fire Retardant for Cellulosic Materials—A Review,” Forests 11 (2020): 755, https://doi.org/10.3390/f11070755.

[13] J. Jin, Q. Dong, Z. Shu, W. Wang, K. He, “Flame Retardant Properties of Polyurethane/Expandable Praphite Composites,” Procedia Engineering 71 (2014): 304–309, https://doi.org/10.1016/j.proeng.2014.04.044.

[14] W.W. Focke, H. Muiambo, W. Mhike, H.J. Kruger, O. Ofosu, “Flexible PVC flame retarded with expandable graphite,” Polymer Degradation and Stability 100 (2014): 63–69, https://doi.org/10.1016/j.polymdegradstab.2013.12.024.

[15] M. Deng, Z. Zhang, J. Sun, X. Liu, H. Li, X. Gu, S. Zhang, “Improving the flame retardancy and water resistance of polypropylene by introducing microcapsule flame retardant system and modified zinc oxide,” Polymer Degradation and Stability 221 (2024): 110668, https://doi.org/10.1016/j.polymdegradstab.2024.110668.

[16] T. Nageswara Rao, T.M. Naidu, M.S. Kim, B. Parvatamma, Y. Prashanthi, B. Heun Koo, “Influence of Zinc Oxide Nanoparticles and Char Forming Agent Polymer on Flame Retardancy of Intumescent Flame Retardant Coatings,” Nanomaterials 10 (2020): 42, https://doi.org/10.3390/nano10010042.

[17] H. Nabipour, X. Wang, L. Song, Y. Hu, “Metal-organic frameworks for flame retardant polymers application: A critical review,” Composites Part A: Applied Science and Manufacturing 139 (2020): 106113, https://doi.org/10.1016/j.compositesa.2020.106113.

[18] Á. Pomázi, A. Toldy, "Development of fire retardant epoxy-based gelcoats for carbon fibre reinforced epoxy resin composites," Progress in Organic Coatings 151 (2021): 106015, https://doi.org/10.1016/j.porgcoat.2020.106015.

[19] A. Toldy, Á. Pomázi, B. Szolnoki, "The effect of manufacturing technologies on the flame retardancy of carbon fibre reinforced epoxy resin composites," Polymer Degradation and Stability 174 (2020): 109094, https://doi.org/10.1016/j.polymdegradstab.2020.109094.

[20] Y. Wang, J. Zhao, M. Xiaojing, "Effect of expandable graphite on polyester resin-based intumescent flame retardant coating," Progress in Organic Coatings 132 (2019): 178–183, https://doi.org/10.1016/j.porgcoat.2019.03.050.

[21] R. Xie, B. Qu, "Thermo-oxidative degradation behaviors of expandable graphite-based intumescent halogen-free flame retardant LLDPE blends," Polymer Degradation and Stability 71 (2001): 395–402, https://doi.org/10.1016/S0141-3910(00)00190-7.

[22] R. Ostrysz, P.A. Penczek, "Expandable graphite as a flame retardant in unsaturated polyester resins," CA2334274A1, 2001, https://patents.google.com/patent/CA2334274A1/en.

[23] A. Dowbysz, M. Samsonowicz, B. Kukfisz, "Modification of Glass/Polyester Laminates with Flame Retardants," Materials (Basel) 14 (2021): 7901. https://doi.org/10.3390/ma14247901.

[24] M. Xiao, F. Yang, S. Im, D.S. Dlamini, D. Jassby, S. Mahendra, R. Honda, E.M.V. Hoek, "Characterizing surface porosity of porous membranes via contact angle measurements," Journal of Membrane Science Letters 2 (2022): 100022, https://doi.org/10.1016/j.memlet.2022.100022.

[25] V. Sharma, S. Agarwal, A. Mathur, S. Singhal, S. Wadhwa, "Advancements in nanomaterial based flame-retardants for polymers: A comprehensive overview," Journal of Industrial and Engineering Chemistry 133 (2024): 38–52, https://doi.org/10.1016/j.jiec.2023.12.010.

[26] H. Chen, X. Tian, J. Liu, "Unsaturated Polyester Resin Nanocomposites Containing ZnO Modified with Oleic Acid Activated by N,N′-Carbonyldiimidazole," Polymers 10 (2018): 362, https://doi.org/10.3390/polym10040362.

[27] D. Karabulut, Ç. Subaşı, H. Çelebi, M.E. Üreyen, A.T. Seyhan, F.K. Özmen, Y. Tezgören, E. Tezgören, Ö.K. Pelen, S. Ersöz, "Synthesis of unsaturated polyester resin with phosphate based flame retardants and investigating their thermal, mechanical, and flame-retardant properties," Journal of Applied Polymer Science 142 (2025): e56442, https://doi.org/10.1002/app.56442.

[28] C. Zhang, M. Shi, Y. Zhang, W. Yang, Z. Jiao, L. Yang, "EG/TPU composites with enhanced flame retardancy and mechanical properties prepared by microlayer coextrusion technology," RSC Advances 9 (2019): 23944–23956, https://doi.org/10.1039/C9RA03653A.